Green Method for Synthesizing Gallium Nitride Nanostructures at Low Temperature

Mahdi Gholampour[*,1,2]**, Amir Abdollah-zadeh**[2]**, Leila Shekari**[3]**, Reza Poursalehi**[2]**, Mahdi Soltanzadeh**[2]

[1] Physics Group, Faculty of Basic Sciences, Imam Ali University, Tehran, Iran

[2] Nanomaterials Group, Department of Materials Engineering, Tarbiat Modares University, P.O. Box 14115-143, Tehran, Iran

[3] Barman International Technology Development Company

Abstract: Gallium nitride (GaN) nanostructures (NS) were synthesized using pulsed direct current plasma enhanced chemical vapor deposition (PDC-PECVD) on quartz substrate at low temperature (600°C). Gallium metal (Ga) and nitrogen (N) plasma were used as precursors. The morphology and structure of the grown GaN NS were characterized by field emission scanning electron microscope (FE-SEM), transmission electron microscopy (TEM) and X-ray diffraction (XRD). The XRD pattern shows that GaN NS were grown in the hexagonal wurtzite-type crystal structure. The optical properties of the grown GaN NS were examined by photoluminescence (PL), UV-visible and Raman spectroscopy. The PL spectroscopy measurements of the grown GaN NS showed blue shifts as compared to the GaN bulk structure. The Raman spectra displayed three Raman active optical phonons at 534 cm^{-1}, 570 cm^{-1} and 730 cm^{-1} due to A_1 (TO), E_2 (high) and A_1 (LO), respectively.

1. INTRODUCTION

GaN structure has Specific optical and physical properties such as, large direct band gap (~3.4 eV) [1, 2], large breakdown electric field (~3.3MV/cm) [3], high thermal conductivity (1.7 W/cm.K) [4] and high electron mobility (1500 cm^2/Vs) [5]. This properties make it as a promising semiconductor for optoelectronic and microelectronic devices [6, 7]. High power transistors, LEDs, gas sensors, multijunction solar cells and solar-blind detectors are some

---

important applications of GaN nanostructures [8–13]. Some different methods of vapor phase deposition to synthesis GaN nanostructure were introduced [14–30]. General methods to grow GaN nanostructures are molecular beam epitaxy (MBE), metal organic chemical vapor deposition (MOCVD) and chemical vapor deposition (CVD) using ultra high vacuum and/or high temperature (up to 1150°C) [14–17, 31, 32]. Recently, GaN powder was used to fabricate GaN nanowires on porous silicon by thermal evaporation at high temperature (~1000°C) [33]. In the above methods, plasma can be used to decrease the growth temperature and enhance chemical reactions [19–25, 34]. The low temperature growth of GaN nanostructure can decrease the amount of impurities [35]. Impurities such as oxygen which associated with GaN nanostructures can reduce the both photoluminescence and Raman spectrum intensity [36]. Optical properties of GaN nanostructures grown on porous silicon, sapphire and quartz substrates can be different, due to residual stresses of lattice mismatches between top-layer and substrates. Growth of GaN nanowires on quartz substrate using ammonia gas, without any catalyst, was reported. Since ammonia is toxic, using N gas is more favorable due to its ease of use and safety. The aim of this study is to synthesize GaN NS via PDC-PECVD on quartz substrate using neither catalyst nor ammonia gas, at low temperature by N_2 and mettalic Ga precursor.. Quartz glass is transparent and do not absorb light itself in the visible, near IR and ultraviolet wavelengths, so in this work, it was used as substrate to study the optical properties of grown GaN NS for optoelectronic applications. The PDC-PECVD technique is simple, flexible and inexpensive at low temperature as compared to other methods to grow GaN NS such as, MOCVD and MBE. Precursors such as, trimethylgallium (TMG), triethylgallium (TEG), Ga_2O_3, gallane (GaH_3) and gallium acetylacetonate ($Ga(acac)_3$) were used as Ga source in several reports, and the NH_3 gas is one of the conventional N sources [15, 17, 37–39]. Using these kinds of precursors may increase the unintentional impurities such as O and C from precursors and N vacancy in GaN crystals. In this research, using Ga and N elements as precursors could help to achieve a high purity GaN production with less N vacancy.

2. EXPERIMENTAL

GaN NS were synthesized using PDC-PECVD system manufactured by Plasmafanavar Co, Iran. The experimental setup is schematically shown in Fig. 1. There was a horizontal quartz tube in a furnace and two parallel stainless steel electrodes were used as anode and cathode in the tube with 4 cm distance. A pulsed DC glow discharge was ignited between two electrodes. A quartz plate of about 10×10 mm^2 in size was used as substrate. The quartz substrate was put

on top of an alumina boat that contained Ga metal. The distance between substrate and Ga source was about 0.8 cm. The alumina boat was placed on the cathode electrode. Metallic Ga and N gas were of high purity of 99.999%. The grown GaN NS were deposited on 3 Torr pressure of reaction chamber. The gas flow rates were controlled by using mass flow controller. Temperature of the furnace was increased at a rate of 35°C/min from room temperature to 600°C and then kept constant for 120 min. H_2, with flow rate of 10 standard cubic centimeters per minute (sccm), was first introduced to quartz tube as a reducing gas to prevent the oxidation of Ga from the surface of electrodes or outgassing of quartz wall. Then temperature of the furnace was increased to 800°C, subsequently. Afterwards the temperature was decreased to 500°C and H_2 gas flow was disconnected by mass flow controller. Ar gas was used as a dilution gas for enhancing the plasma density to improve the decomposition of N gas [40]. Nitrogen and Ar gas were introduced at 500°C with flow rates of 130 and 100 sccm, respectively. Voltage and current which were applied to the electrodes were 500 V and 2 A, respectively, at a frequency of 10 kHz. Nitrogen plasma was generated between the electrodes (so that alumina boat placed in the ambient plasma) to produce sufficient active N radicals and ions to create GaN NS with low nitrogen vacancy. Morphology and compositions of the samples were characterized using field emission scanning electron microscopy (SIGMA/VP ،ZEISS) coupled with energy-dispersive X-ray spectroscopy (x-Max oxford) and transmission electron microscopy (Zeiss - EM10C - 80 KV).
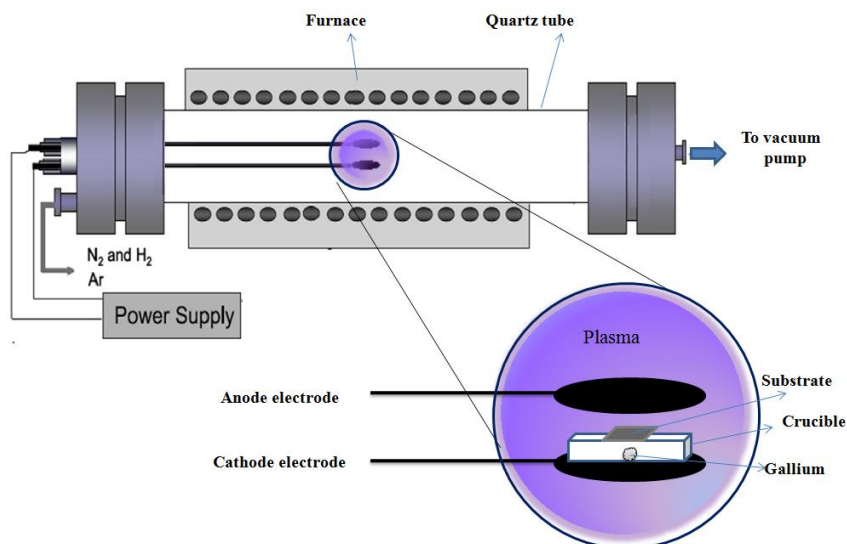

Fig. 1. Schematic diagram of PDC-PECVD experimental set-up [41].

The phase and structural characterizations of GaN NS were examined using X-ray diffraction (Philips Analytical, X'PERT MPD) with cobalt radiation Co, Kα at λ=1.7889Å. The active Raman mods and presence of defects of GaN NS were investigated using Raman spectroscopy with a 532 nm polarized Nd:YLF laser as the exiting source. Photoluminescence (PL) spectrum (Varian Cary Eclipse Fluorescence Spectrophotometer) was measured at room temperature. UV-visible absorption and transmission spectra of GaN NS were recorded with a UV-visible spectrophotometer at room temperature.

3. RESULTS AND DISCUSSION

Fig. 2 show FE-SEM images of grown worm-like GaN NS on quartz substrate in two different magnifications. The grown GaN NS are of different grain sizes which are about 60-100 nm (measured using ImageJ software). Fig. 2c demonstrates EDS result of samples that indicate the presence of Ga and N which are from GaN NS, and Si and O elements that are attributed to the quartz substrate.
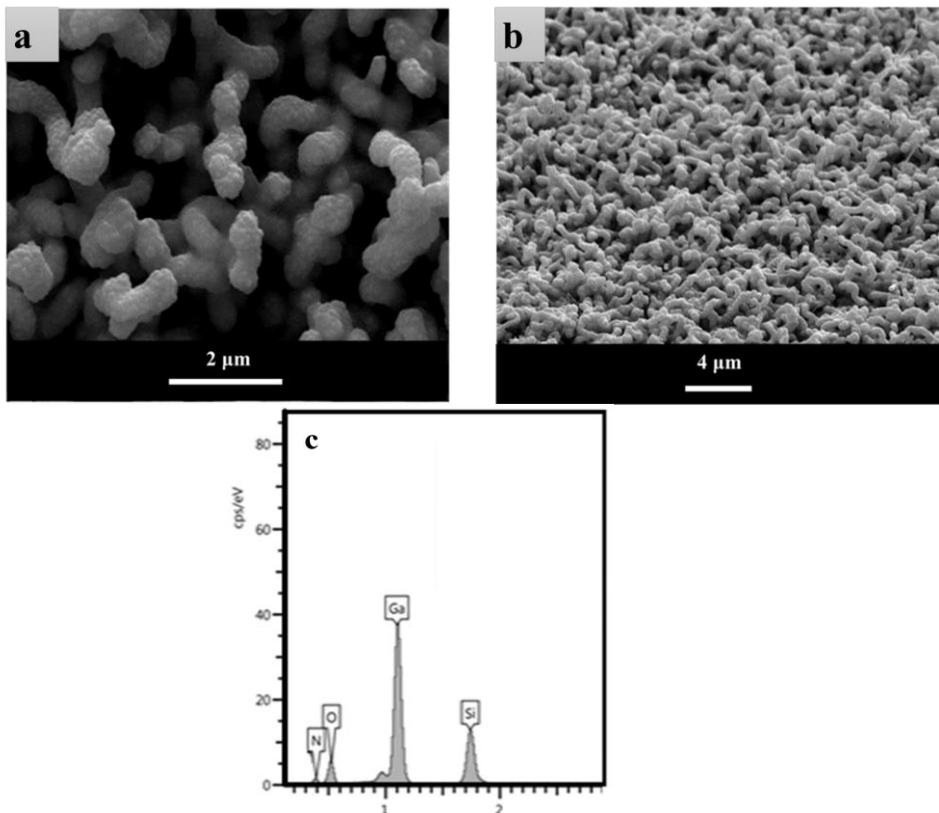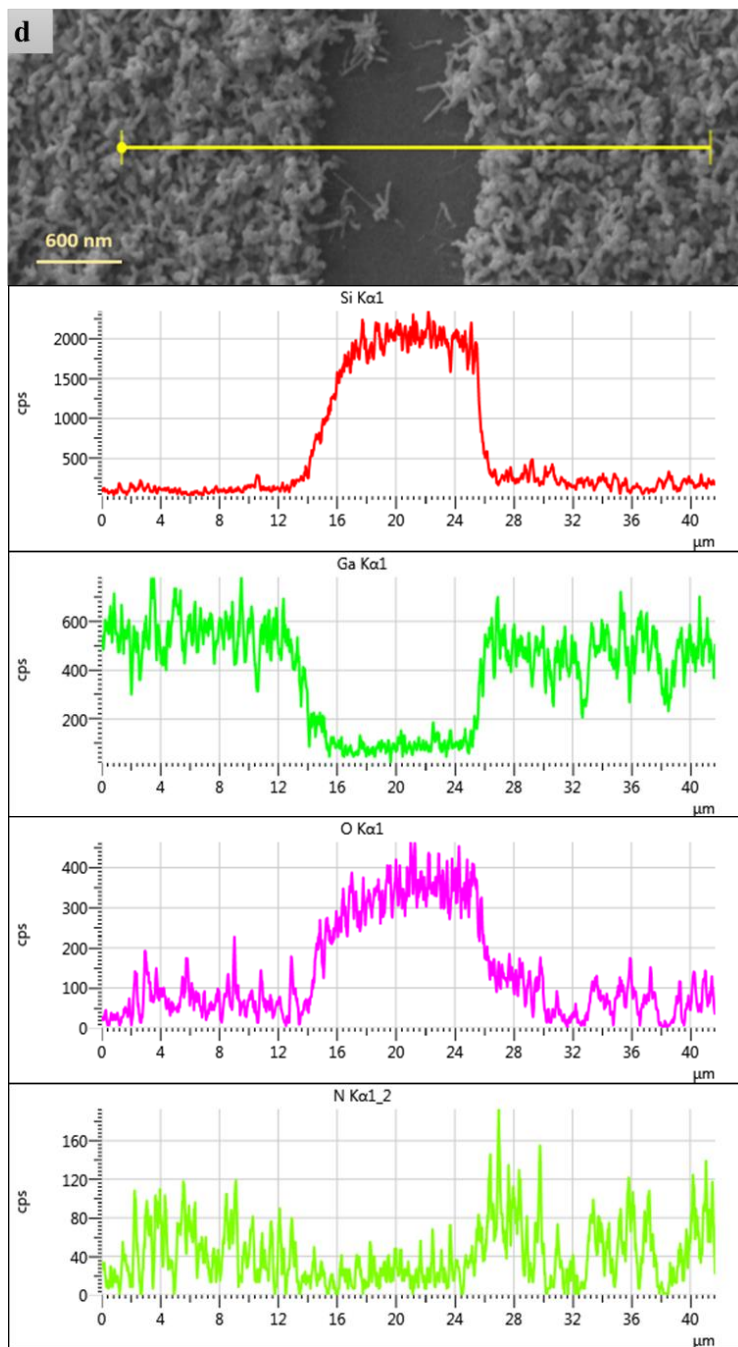
Fig. 2. (a and b) FESEM images, (c) EDS spectrum, and (d) line EDS analysis, of GaN NS.

The line EDS analysis of the grown samples in Fig. 2d indicates that there are Ga and N elements on quartz substrate. It can be seen from Fig. 2d that the amount of Ga and N are quite high in deposition region. There is a crack in the GaN NS deposition which is due to thermal expansion coefficient between the grown GaN and the quartz substrate or nanostructure island growth[26]. The amount of N in the crack is relatively tangible due to N ions penetrating into the substrate. Penetrating of N is achieved by bombarding the quartz substrate with energetic N ions in plasma. The coordination between the N and Ga curves can indicate large part of the N is combined with Ga in GaN NS.Fig. 3 presents the TEM image of GaN NS which were deposited by PDC-PECVD technique on quartz substrate. The TEM image shows that the density of grown GaN NS is partially low and coalescence growth of GaN NS occurred at this growth process. This image reveals distinct tuber-like shapes of the grown GaN NS that is consistent with the FESEM images in size and shape. As obviously can be seen from Fig. 4 the XRD pattern illustrates the growth of wurtzite GaN NS. Several GaN crystal plans including (100), (002), (101), (102), (110), (103), (200) and (112) can be observed. According to reference code 01-074-0243, GaN was grown in hexagonal wurtzite structure with lattice constants of a=3.188 Å and c=5.168 Å and lattice angles of $\alpha = \beta = 90°$ and $\gamma = 120°$ which are consistent with the bulk GaN. The lattice parameters of bulk GaN were reported to be about a=b=3.189 and c=5.185. These differences can be due to internal stresses in the grown NS. Three strongest diffraction peaks, (100), (002) and (101) are placed at 2theta angle of 37.89°, 40.57° and 43.17 °, respectively. These peaks show that the GaN NS have grown in both directions of a-axis (100) and c-axis (002).
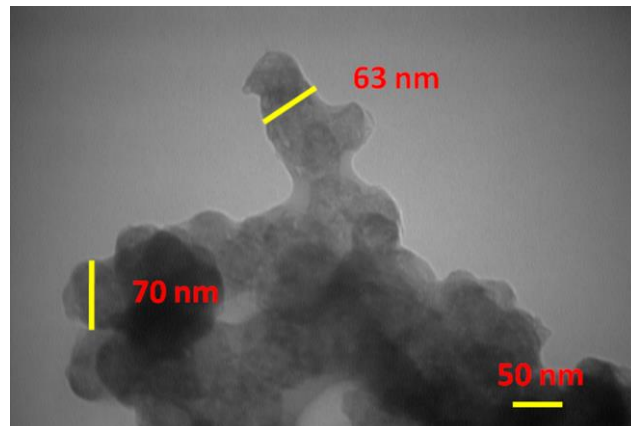

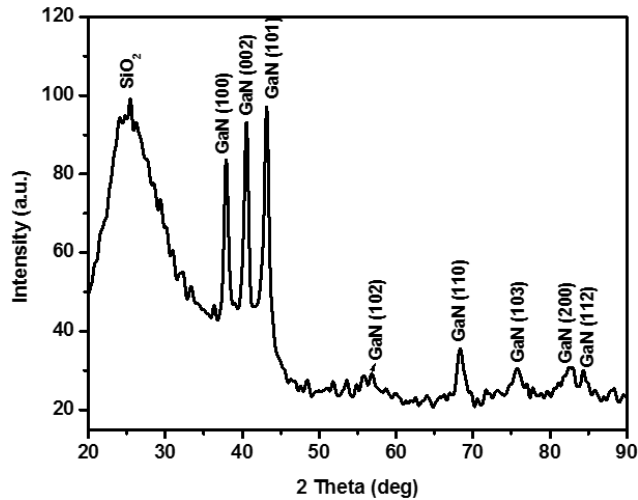**Fig. 3.** TEM image of GaN NS were grown on quartz substrate.

Fig. 4. X-ray diffraction of wurtzite GaN NS were grown by PDC-PECVD method.

There is a broad peak from polymorphs structure of SiO_2 substrate at about 25° (reference code 01-089-3606). A broad peak of (101) at 43.17° width full with at half maximum (FWHM) intensity of 2theta=0.501° is detected and confirms that deposited GaN is of nano crystalline.

PL spectrum of the GaN NS is shown in Fig. 5a. The measurement was conducted at room temperature in the region of 200–410 nm using Xenon lamp as the PL source with excitation wavelength of 260 nm. The broad PL emission peak includes a UV light emission with its maximum intensity centered at ~ 359 nm is clearly observed. The energy gap of the grown GaN NS is 3.45 eV, which is higher than that of bulk GaN [42]. The PL data of the samples was recorded at 45° relative to the excitation beam. There is a blue shift of ~50 meV in the energy gap of the grown GaN NS as compared to the bulk [43]. The shift induced by quantum confinement effect, residual stresses and thermal effects of grown GaN NS [44–46]. The broad main peak of the PL spectrum is around 359 nm which could be due to the defects incorporation in the NS or distribution of stress-strain in NS that affects the excitonic gap for instance by affecting the donor–bound electron and hole pair [18, 47, 48]. The broad PL peak shows that the GaN NS can absorb wavelengths of 350-370 nm and it is suitable for solar cell application. Fig. 5b illustrates the polarized Raman scattering of GaN NS grown on quartz substrate and bare quartz at room temperature. Four Raman active modes were predicted for GaN single crystal including A_1, E_1 and $2E_2$ (E_2^H and E_2^L), H and L means higher-frequency and lower frequency branches, respectively. The A_1 and E_1 modes split into longitudinal optical (LO) and transverse optical (TO) modes [49].
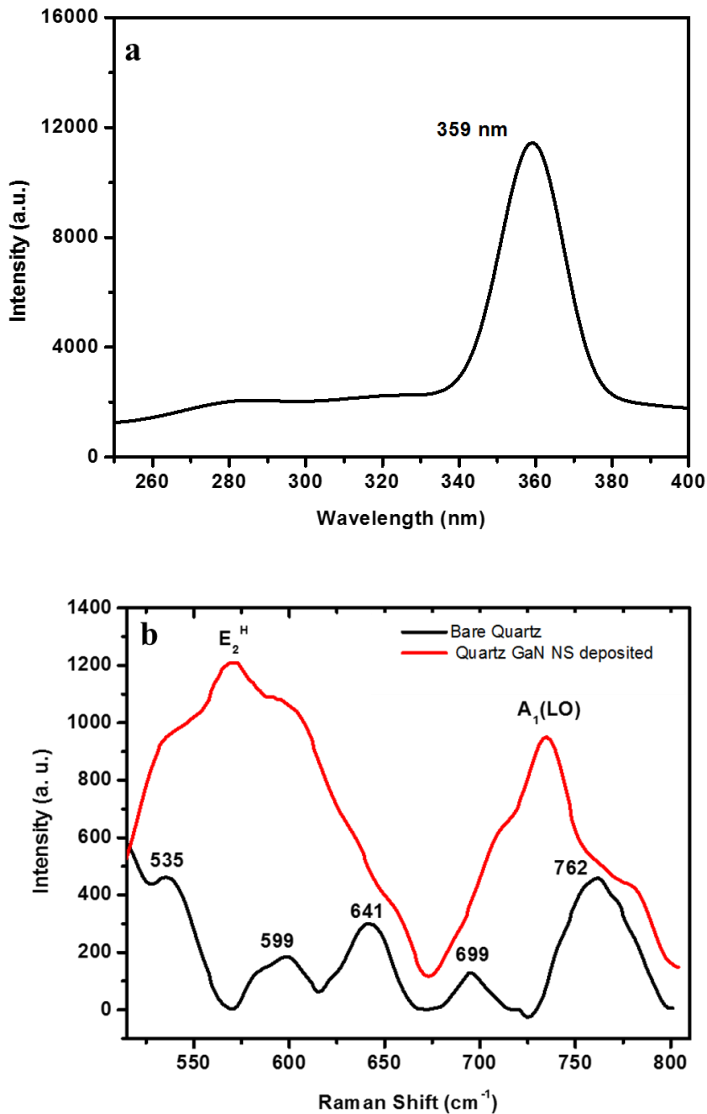
Fig. 5. (a) Photoluminescence spectrum, and (b) Raman spectrum, of GaN NS deposited on quartz substrate.

There are five peaks at 535, 599, 641, 692 and 762 cm^{-1} attributed to different bending modes of Si and O in SiO$_2$ of uncoated quartz [50, 51]. The Raman active phonon bands of GaN NS near 570 and 730cm^{-1} are assigned of E$_2^H$ and A1 (LO), respectively. A1(TO) placed at about 534 cm^{-1} and can be overlapped with the 535 cm^{-1} of quartz. A1 and E$_1$ are polar modes, and then E$_1$ is null

because polarized Raman spectrum is recorded as the polarization direction of the incident light for NS [52, 53]. Size effects, tensile strains, formation of coupled Plasmon-phonon mode, polarization dependences, residual stresses, thermal effects, vacancies and defects play an important role in the shift of Raman modes [45, 52, 54, 55]. As for A_1(TO), E_2^H and A_1(LO) modes, the grown GaN shows blue shifting of 9, 2 and 6 cm-1, as compared to 525, 568 and 724 cm^{-1}, respectively [49, 52].. These results are in good agreement with the Raman spectrum of GaN from refs. [49, 52, 56].

The optical transmission spectrum of GaN NS is shown in Fig. 6a and is measured over a wavelength rang of 225 to 460 nm. The spectrum illustrated the strong cut off at ~360 nm. This result is compatible with the photoluminescence spectrum in Fig. 5a. Fig. 6a demonstrates that transmittance of the GaN NS increases as the wavelength increases. The optical transparency of GaN NS grown on quartz substrate in visible wavelengths is about 80%.

The energy band gap of GaN NS is determined from optical transmission spectrum as shown in Fig. 6a. Tauc model widely used for description and calculation of semiconductors optical band gaps [57, 58]. According to the Tauc relation, the absorption coefficient α for direct band gap semiconductors is described by:

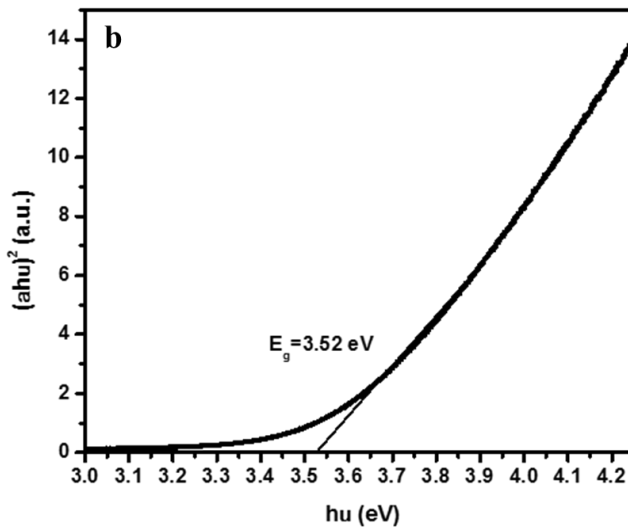$$(\alpha h\upsilon)^2 = A(h\upsilon - E_g)$$
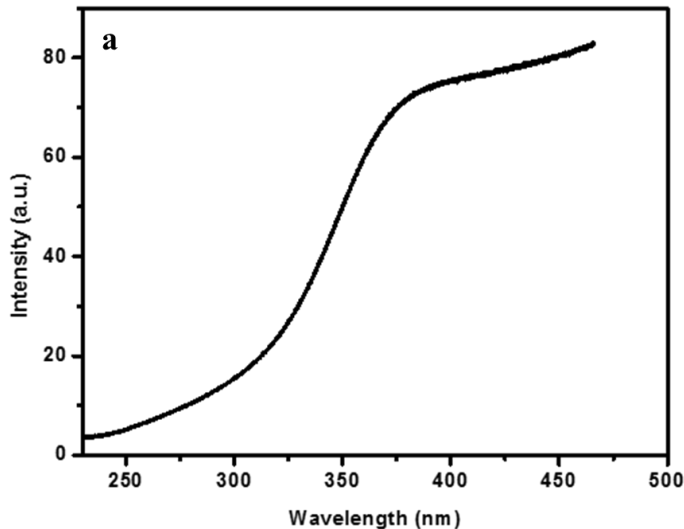
Fig. 6. (a) Optical transmittance spectrum of the grown GaN NS and (b) the square product of absorption coefficient and incident photon energy as a function of photon energy for the GaN NS.

where $h\upsilon$ is incident photon energy and constant A is depends on transition. The square product of the absorption coefficient and incident photon energy is plotted versus incident photon energy is shown in Fig. 6b. The curve demonstrates a section of straight line in limited region above band gap energy. By extrapolation of straight region of the curve or drawing tangent line to the curve, the intersection point of tangent line and photon energy axis gives the band gap energy of GaN NS. According to Fig. 6b the band gap of the grown GaN NS is 3.52 eV. This value of band gap is in excellent agreement with the photoluminescence broad emission peak, which is around the wavelength of 359nm as demonstrated in Fig. 5a. In addition this band gap value corresponds well with the optical transmission spectrum of GaN NS as shown in Fig. 6b.

4. CONCLUSION

To summarize, the GaN NS were synthesized on quartz plate at low temperature of 600°C by PDC- PECVD method using pure metallic Ga and N plasma as precursors, without any catalyst. The XRD, FE-SEM confirmed the synthesis of GaN NS of wurtzite nanostructure of 60-100 nm. According to the TEM image, density of the grown sample was relatively low. The results of optical characterizations of the deposited GaN NS such as photoluminescence

and Raman spectroscopes showed blue shifts of PL data and Raman spectra. The transmission spectrum of GaN NS illustrated the strong cut off around 360 nm. According to PL result, the GaN NS can be used for solar cell application. The optical transparency of these samples at visible wavelengths is about 80%. The band gap energy of GaN NS has been determined about 3.52 eV by transmission spectrum, which is compatible with PL broad emission peak. It was shown that the quartz substrate have a significant role in the growth process of GaN NS. Furthermore, the GaN NS were formed in low temperature by employing N plasma.

REFERENCES

[1] Pankove JI. *Luminescence in GaN*. J Lumin. (1973) .

[2] Pankove JI. *Luminescent properties of GaN*. Solid State Commun. (1970) .

[3] Kaun SW. *Molecular beam epitaxy for high-performance Ga-face GaN electron devices*. Semicond Sci Technol. 28 (7) (July 2013) 074001.

[4] Shibata H. *High Thermal Conductivity of Gallium Nitride (GaN) Crystals Grown by HVPE Process*. Mater Trans. 48 (10) (2007) 2782–2786.

[5] Pengelly RS. *A review of GaN on SiC high electron-mobility power transistors and MMICs*. IEEE Trans Microw Theory Tech. 60 (6) (2012) 1764–1783.

[6] Du Y. *Electronic structure and optical properties of zinc-blende GaN*. Optik (Stuttg). 123 (December 2012) 2208–2212.

[7] Kente T. *Gallium nitride nanostructures: Synthesis, characterization and applications*. J Cryst Growth. 444 (2016) 55–72.

[8] Saron KM a. *Self-catalyst growth of novel GaN nanowire flowers on Si (111) using thermal evaporation technique*. Mater Chem Phys. 139 (2)–(3) (May 2013) 459–464.

[9] Saron KMA. *NH3-Free growth of GaN nanostructure on n-Si (111) substrate using a conventional thermal evaporation technique*. J Cryst Growth. 349 (June 2012) 19–23.

[10] Yasuhiko A. *Progress in GaN-based nanostructures for blue light emitting quantum dot lasers and vertical cavity surface emitting lasers*. IEICE Trans Electron. E83 (2000) 564–572.

[11] Kang MS. *Gallium nitride nanostructures for light-emitting diode applications*. Nano Energy. 1 (3) (May 2012) 391–400.

[12] Gopalakrishnan M. *Structural and optical properties of GaN and InGaN nanoparticles by chemical co-precipitation method*. Mater Res Bull. 47 (11) (2012) 3323–3329.

[13] Gholampour M. *Synthesis of Serrated GaN Nanowires for Hydrogen Gas Sensors*

Applications by Plasma-Assisted Vapor Phase Deposition Method. J Nanostructures. 7 (3) (2017) 200–204.

[14] Schuster F. *Self-assembled GaN nanowires on diamond*. Nano Lett. 12 (May 2012) 2199–2204.

[15] Im MK. *Metalorganic Molecular Beam Epitaxy of GaN Thin Films on a Sapphire Substrate*. Jpn J Appl Phys. 39 (2000) 6170–6173.

[16] Grant VA. *Optimization of RF plasma sources for the MBE growth of nitride and dilute nitride semiconductor material*. Semicond Sci Technol. 22 (2) (2007) 15.

[17] Jeong JK. *Improvement in the Crystalline Quality of Epitaxial GaN Films Grown by MOCVD by Adopting Porous 4H-SiC Substrate*. Electrochem Solid-State Lett. 7 (2004) C43–C45.

[18] Shekari L. *High-quality GaN nanowires grown on Si and porous silicon by thermal evaporation*. Appl Surf Sci. 263 (2012) 50–53.

[19] Zhu CF. *Influence of double buffer layers on properties of Ga-polarity GaN films grown by rf-plasma assisted molecular-beam epitaxy*. Mater Lett. 57 (2003) 2413–2416.

[20] Mata R. *Nucleation of GaN nanowires grown by plasma-assisted molecular beam epitaxy: The effect of temperature*. J Cryst Growth. 334 (1) (2011) 177–180.

[21] Hou W. *Synthesis of GaN Core-shell Nanowires by Plasma-Enhanced Chemical Vapor Deposition*. Chem Eng. (2010) 8–9.

[22] Hou WC. *Nucleation control for the growth of vertically aligned GaN nanowires*. Nanoscale Res Lett. 7 (January 2012) 1–6.

[23] Nagata T. *Hydrogen Effect on Near-Atmospheric Nitrogen Plasma Assisted Chemical vapor Deposition of GaN Film Growth*. J Appl Phys. 105 (2009) 536–541.

[24] Sani R a. *Growth of GaN " lm on a-plane sapphire substrates by plasma-assisted MOCVD*. 221 (2000) 311–315.

[25] Qiaoqin Y. *Plasma-enhanced Deposition of Nano-Structured Carbon Films*. Plasma Sci Technol. 7 (February 2005) 2660–2664.

[26] Gholampour M. *Synthesis of GaN Nanoparticles by DC Plasma Enhanced Chemical Vapor Deposition*. 829 (2014) 897–901.

[27] Cai XM. *CVD growth of InGaN nanowires*. J Alloys Compd. 467 (1) (2009) 472–476.

[28] Ng DKT. *Selective growth of gallium nitride nanowires by femtosecond laser patterning*. J Alloys Compd. 449 (1)–(2) (January 2008) 250–252.

[29] Huang E. *A simple synthesis of Ga 2 O 3 and GaN nanocrystals*. RSC Adv. 7 (76) (2017) 47898–47903.

[30] Rabiee Golgir H. *Fast Growth of GaN Epilayers via Laser-Assisted Metal–Organic Chemical Vapor Deposition for Ultraviolet Photodetector Applications*. ACS Appl Mater Interfaces. 9 (25) (2017) 21539–21547.

[31] Liu K-W. *Growth of gallium nitride on silicon by molecular beam epitaxy incorporating a chromium nitride interlayer*. J Alloys Compd. 511 (1) (January 2012) 1–4.

[32] Cui J. *Morphology and growth mechanism of gallium nitride nanotowers synthesized by metal–organic chemical vapor deposition*. J Alloys Compd. 563 (June 2013) 72–76.

[33] Shekari L. *Fabrication of GaN nanowires on porous GaN substrate by thermal evaporation*. Mater Sci Semicond Process. 16 (2) (2013) 485–488.

[34] Beh KP. *The growth of III–V nitrides heterostructure on Si substrate by plasma-assisted molecular beam epitaxy*. J Alloys Compd. 506 (1) (September 2010) 343–346.

[35] Butcher KSA. *Optical and structural analysis of GaN grown by remote plasma enhanced laser induced chemical vapour deposition*. phys stat sol. 503 (1) (2002) 499–503.

[36] Saron KMA. *Enhanced ultraviolet emission in photoluminescence of GaN film covered by ZnO nanoflakes*. J Lumin. 134 (2013) 266–271.

[37] Qaeed M a. *Cubic and hexagonal GaN nanoparticles synthesized at low temperature*. Superlattices Microstruct. 64 (December 2013) 70–77.

[38] Nagata T. *GaN film fabrication by near-atmospheric plasma-assisted chemical vapor deposition*. Jpn J Appl Phys. 46 (No. 2) (2007) 43–45.

[39] Timoshkin AY. *DFT modeling of chemical vapor deposition of GaN from organogallium precursors. 2. structures of the oligomers and thermodynamics of the association processes*. J Phys Chem A. 105 (2001) 3249–3258.

[40] Chang Y-K. *Synthesis and characterization of indium nitride nanowires by plasma-assisted chemical vapor deposition*. Mater Lett. 63 (August 2009) 1855–1858.

[41] Gholampour M. *A catalyst free method to grow GaN nanowires on porous Si at low temperature*. Ceram Int. 41 (10) (2015) 13855–13860.

[42] Torii K. *Reflectance and emission spectra of excitonic polaritons in GaN*. Phys Rev B. 60 (7) (August 1999) 4723–4730.

[43] Wei X. *Synthesis and characterization of GaN nanowires by a catalyst assisted chemical vapor deposition*. Appl Surf Sci. 257 (September 2011) 9931–9934.

[44] Yoon J-W. *Quantum confinement effect of nanocrystalline GaN films prepared by pulsed-laser ablation under various Ar pressures*. Thin Solid Films. 471 (1) (2005) 273–276.

[45] Matoussi A. *Luminescent properties of GaN films grown on porous silicon*

substrate. J Lumin. 130 (3) (March 2010) 399–403.

[46] Oh TS. *Spatial stress distribution and optical properties of GaN films grown on convex shape-patterned sapphire substrate by metalorganic chemical vapor deposition*. J Alloys Compd. 509 (6) (February 2011) 2952–2956.

[47] Shekari L. *Structural characterizations of GaN nanowires grown on Si (111) substrates by thermal evaporation*. Mater Lett. 114 (January 2014) 140–143.

[48] Chin AH. *Photoluminescence of GaN nanowires of different crystallographic orientations*. Nano Lett. 7 (2007) 626–631.

[49] Harima H. *Properties of GaN and related compounds studied by means of Raman scattering*. J Phys Condens Matter. 14 (2002) 967–993.

[50] Dračínský M. *Ab initio modeling of fused silica, crystal quartz, and water Raman spectra*. Chem Phys Lett. 512 (1)–(3) (August 2011) 54–59.

[51] Hnnoerson S. *silicate Raman spectra of gallium and germanium substituted vaiiations in intermediate range order Uniuersitry*. Am Mineral. 70 (1985) 946–960.

[52] Livneh T. *Polarized Raman scattering from single GaN nanowires*. Physcal Rev B. 74 (2006) 035320.

[53] Sekine T. *Surface Phonons Studied by Raman Scattering in GaN Nanostructures*. J Phys Soc Japan. 86 (7) (2017) 74602.

[54] Munawar Basha S. *Effect of growth temperature on gallium nitride nanostructures using HVPE technique*. Phys E Low-Dimensional Syst Nanostructures. 44 (9) (2012) 1885–1888.

[55] Yadav BS. *Highly oriented GaN films grown on ZnO buffer layer over quartz substrates by reactive sputtering of GaAs target*. Thin Solid Films. 517 (2) (November 2008) 488–493.

[56] Nyk M. *Synthesis, structure and optical properties of GaN nanocrystallites*. Mater Sci Semicond Process. 8 (4) (August 2005) 511–514.

[57] Chen R. *Top-gate thin-film transistors based on GaN channel layer*. Appl Phys Lett. 100 (2) (2012) 022111.

[58] Souri D. *Band gap determination by absorption spectrum fitting method (ASF) and structural properties of different compositions*. J Non Cryst Solids. 355 (31)–(33) (2009) 1597–1601.